

The Influence of Temperature Gradient on Thin Plates Bending

Vesna Milošević-Mitić

Professor
University of Belgrade
Faculty of Mechanical Engineering

Ana Petrović

Assistant Professor
University of Belgrade
Faculty of Mechanical Engineering

Nina Andelić

Professor
University of Belgrade
Faculty of Mechanical Engineering

Miloš Jovanović

Teaching Assistant
University of Belgrade
Faculty of Mechanical Engineering

Within the theory of thermo-elasticity, the temperature field of thin plates is commonly defined via two parameters: temperature in the mid-plane and linear temperature gradient normal to the mid-plane. First, the paper analytically proves the justification of that assumption in machine structures. Then, in an analytical closed form, applying the integral transformation method, the thin plate deflection caused by a constant temperature gradient is defined. It is shown that, in that case, the plate deflection does not depend on its thickness but only on the plate dimensions in the mid-plane. Analytically defined values are compared to corresponding values obtained by applying the thin plate finite element, where the temperature field is described using the two mentioned parameters. This finite element is defined and programmed within the Komips program package. The influence of the temperature gradient on the behavior of constructions mostly depends on the type of material. That is why the behavior of some structural elements made of brass, steel, and concrete is analyzed in this paper.

Keywords: temperature, temperature gradient, plate, deflection, stress, finite element, steel, concrete

1. INTRODUCTION

A large number of machine structures, such as steam boilers, heat exchangers, furnaces, chemical reactors, evaporators, engine parts, etc., represent thermally loaded structures of complex geometry. In the design and analysis of this type of structure, the finite element method is mainly used today. Due to the complexity of the geometry, 2D and 3D finite elements are mostly used to create calculation models, which are assigned a thermo-mechanical load.

The analysis of stress due to pressure and thermal loads in structures such as fire-tube boilers shows that thermal stress is not of lower order compared to stress due to pressure loads [1,2]. The effects of the surface roughness of the friction facing the generated heat and temperature fields are investigated in [3]. A finite element model was developed to study the thermal behavior of a disc clutch system. The importance of research [4] is given to the variation of temperature along the length of the fins. The presented methodology involved 3D rectangular fin modeling and the creation of surf elements for applying the boundary conditions and source temperature obtained in the state of thermal contours.

In some processes, such as the laser formation of thin plates, the temperature gradient mechanism is very important. Laser forming is a technique that forms sheet metal by means of induced non-uniform thermal stress. So, in paper [5], the temperature gradient mechanism is studied to obtain the deformation of a plate in the laser forming process. Thermal stress is significant in welding processes, too, and in [6], a mathematical

model was developed to predict the temperature distribution and stress concentration at localized nodal points.

Thermal load acting on thin plates can provide their bending, buckling, and curling. A theoretical model for the nonlinear analysis of thin rectangular plates subjected to mechanical load and to non-uniform thermal gradients is discussed in [7], and several numerical examples are presented. The influence of thermal gradient is very significant in the analysis of structures with low heat conduction coefficients, such as structures of silicon materials or concrete. Thermoelastic vibrations of functionally graded plates of silicon material subjected to thermal load are shown in [8]. A finite element model for unsteady phased thermal-stress analysis of gravity dams made of a special concrete mixture with low cement content is presented in [9]. Thin-walled plates and tubes were experimentally investigated to obtain the effects of thermal loads, and appropriate finite element models were developed [10].

Machine structures are mainly built of steel whose heat conduction is comparatively high and amounts to approx. 50 W/mK. The objective of this paper is first to analytically show that temperature distribution in thin-walled structures is mainly linear across their thickness. Therefore, for further analysis of thin-walled thermally loaded structures, the simplest way is to use a 2D finite element for a thin plate, which has the possibility of assigning temperature in the mid-plane as well as temperature gradient normal to the plate mid-plane. Such finite element was programmed within the KOMIPS package [11], and its verification is presented by applying analytical calculations.

2. TEMPERATURE DISTRIBUTION ACROSS THE PLATE THICKNESS

A general differential equation of heat conduction for uncoupled thermo-elasticity problems reads [12]

Received: May 2023, Accepted: December 2023

Correspondence to: Vesna Milošević-Mitić

Faculty of Mechanical Engineering,

Kraljice Marije 16, 11120 Belgrade 35, Serbia

E-mail: vmilosevic@mas.bg.ac.rs

doi: [10.5937/fme2401128M](https://doi.org/10.5937/fme2401128M)

© Faculty of Mechanical Engineering, Belgrade. All rights reserved

$$\left(\nabla^2 - \frac{1}{\kappa} \frac{\partial}{\partial t} \right) \theta(x, y, z, t) = -\frac{W(x, y, z, t)}{\lambda}, \quad (1)$$

where κ is the coefficient of thermal intensity, λ is the heat conduction coefficient, ∇^2 is the Laplace operator, and t is the time.

The temperature field is presented as $\theta=T-T_0$ [$^\circ$ C, K], where T_0 is the plate's temperature in its natural state. The quantity of heat generated in a unit volume and unit time is presented as $W(x_1, x_2, x_3, t)$.

Observe part of the plate of thickness h as shown in Fig. 1. Assume that the plate temperature changes only in the direction of axis z and that the temperatures on the upper and lower surfaces are constant. Since we are interested here only in temperature change across the plate thickness, let us choose boundary and initial values in the form as follows:

$$\begin{aligned} \theta(z=0, t) &= \theta_0, \\ \theta(z=h, t) &= 0, \\ \theta(z, t=0) &= 0, \quad 0 < z < h. \end{aligned} \quad (2)$$

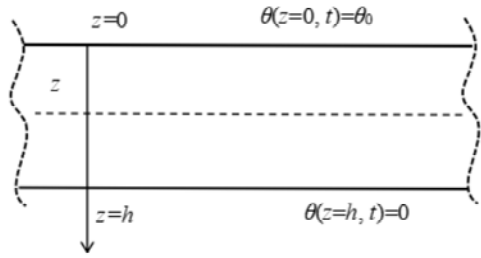


Figure 1. Plate of thickness h with constant temperatures on the upper and lower surfaces

The problem of this type is often encountered in engineering practice, and a corresponding differential equation is of the form

$$\left(\frac{\partial^2}{\partial z^2} - \frac{1}{\kappa} \frac{\partial}{\partial t} \right) \theta(z, t) = 0. \quad (3)$$

In accordance with specified boundary and initial conditions, Eq. (3) is analytically solved in the simplest manner by applying the finite Fourier sine transformation of the form

$$\theta_s(k, t) = \int_0^h \theta(z, t) \sin \alpha_k z dz, \quad \alpha_k = \frac{k\pi}{h}. \quad (4)$$

Since

$$\begin{aligned} \int_0^h \frac{d^2 \theta(z, t)}{dz^2} \sin \alpha_k z dz &= \\ &= \alpha_k^2 \left[(-1)^{k+1} \theta(z=h) + \theta(z=0) \right] - \alpha_k^2 \theta_s(k, t), \end{aligned}$$

after applying this transformation, Eq. (4) has the form

$$\alpha_k \theta_s(k, t) H(t) - \alpha_k^2 \theta_s(k, t) - \frac{1}{\kappa} \frac{\partial}{\partial t} \theta_s(k, t) = 0, \quad (5)$$

where $H(t)$ is the Heaviside function. Applying the Laplace transformation defined by the expression

$$\theta_s^*(k, p) = \int_0^\infty \theta_s(k, t) e^{-pt} dt, \quad (6)$$

the transformed function is obtained

$$\theta_s^*(k, p) = \frac{\kappa \alpha_k \theta_0}{(\kappa \alpha_k^2 + p) p}. \quad (7)$$

Inverse transformations must be applied to obtain the analytical closed-form solution. Applying the inverse Laplace transformation, the expression obtained is

$$\theta_s(k, t) = \frac{\theta_0}{\alpha_k} \left(1 - e^{-\kappa \alpha_k^2 t} \right) H(t), \quad (8)$$

so that the solution of a specified problem in the form of infinite order reads

$$\begin{aligned} \theta(z, t) &= \frac{2\theta_0}{h} \sum_{k=1}^{\infty} \frac{\left(1 - e^{-\kappa \alpha_k^2 t} \right)}{\alpha_k} H(t) \sin \alpha_k z, \quad 0 < z < h, \\ \theta|_{z=0} &= \theta_0, \quad \theta|_{z=h} = 0. \end{aligned} \quad (9)$$

Let us perform the analysis of the expression (9). Until a steady state is reached, the plate temperature changes in accordance with the presented exponential law. When the steady state is achieved, the expression becomes

$$\begin{aligned} \theta(z, t) &= 2\theta_0 \sum_{k=1}^{\infty} \frac{\sin \alpha_k z}{k\pi}, \quad 0 < z < h, \\ \theta|_{z=0} &= \theta_0, \quad \theta|_{z=h} = 0. \end{aligned} \quad (10)$$

Let us define analytically the temperature in the plate mid-plane ($z=h/2$). The temperature can be shown via a comparatively simple infinite-order

$$\theta\left(\frac{h}{2}, t\right) = 2\theta_0 \sum_{k=1}^{\infty} \frac{\sin \frac{k\pi}{2}}{k\pi} = \frac{2\theta_0}{\pi} \sum_{i=0}^{\infty} \frac{(-1)^{i-1}}{2i+1}. \quad (11)$$

The obtained alternative order is convergent according to the Leibniz criterion and corresponds to the alternative order of the function arctg(x)

$$\text{arctg}(x) = \sum_{i=0}^{\infty} \frac{(-1)^{i-1}}{2i+1} x^{2i+1}, \quad |x| \leq 1, \quad (12)$$

so that

$$\theta\left(\frac{h}{2}, t\right) = 2\theta_0 \sum_{k=1}^{\infty} \frac{\sin \frac{k\pi}{2}}{k\pi} = \frac{2\theta_0}{\pi} \text{arctg} 1 = \frac{\theta_0}{2}. \quad (13)$$

When a steady state is reached, the temperature in the mid-plane equals half of the sum of the temperatures on the upper and lower surfaces of the thin plate $[\theta(z=0) + \theta(z=h)]/2$. Its change is linear.

A numerical example will be used to show it. Observe the plate with a thickness of $h=100$ mm, whose lower surface temperature equals the environment

temperature, and let the upper surface temperature be higher by 8°C . The plate used is steel plate, while corresponding characteristics necessary for calculations are given in Table 1: thermal conductivity λ , the coefficient of thermal expansion α_t , material density ρ , thermal diffusion coefficient κ , and Poisson's ratio v .

Table 1. Material characteristics of carbon steel

λ [W/mK]	α_t [K $^{-1}$]	ρ [kg/m 3]	κ [m 2 /s]	v
50.2	$1.2 \cdot 10^{-5}$	$7.85 \cdot 10^3$	$1.36 \cdot 10^{-5}$	0.3

To illustrate the rate of establishing a steady state, in accordance with Eq. (9), let us draw a corresponding diagram of the temperature change over time across the plate thickness. It can be seen from the diagram in Fig. 2 that after about 4 minutes, a linear distribution of temperature is established across the plate thickness, so in this case, it does not make any sense to consider a dynamic problem.

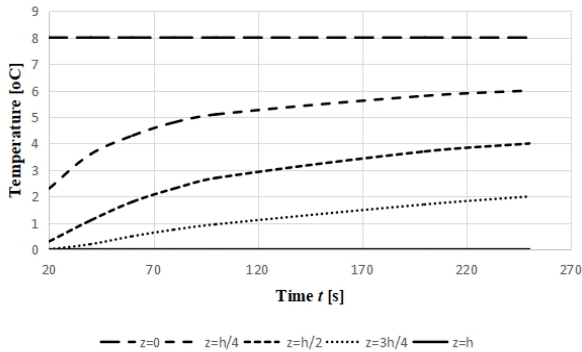


Figure 2. Temperature changes across plate thickness depending on time

Further calculations will involve the observation of the thin plate behavior as influenced by the linear temperature gradient in the quasi-steady state.

3. THIN PLATE DEFORMATION INFLUENCED BY LINEAR TEMPERATURE GRADIENT

Analytical calculations of thin plates commonly involve introducing the assumption that temperature changes linearly across the plate thickness. As shown in the previous part of the paper, this assumption is completely justifiable for the majority of thermally loaded machine structures. Using the Cartesian coordinate system presented in Fig. 3, the temperature field $\theta(x_1, x_2, x_3, t)$ can be described using values τ_0 and τ_1 as [12]

$$\theta(x_1, x_2, x_3, t) = \tau_0(x_1, x_2, t) + x_3 \tau_1(x_1, x_2, t) \quad (14)$$

where τ_0 [K, $^{\circ}\text{C}$] is the mid-plane temperature, and τ_1 [K/m] represents the temperature gradient normal to the mid-plane. The temperature in the mid-plane causes only membrane stresses, which can be most readily determined by applying the finite element method. Here, only the influence of temperature gradient on the thin plate bending will be analytically determined.

The differential equation that describes the dynamic change of the plate deflection (displacement w in the direction of axis x_3) is shown by the expression [13]

$$D\nabla_1^4 w + D(1+v)\alpha_t \nabla_1^2 \tau_1 + \rho h \ddot{w} - \frac{\rho h^3}{12} \nabla_1^2 \ddot{w} = 0, \quad (15)$$

where D is a common value of the plate bending stiffness

$$D = \frac{Eh^3}{12(1-v)^2}.$$

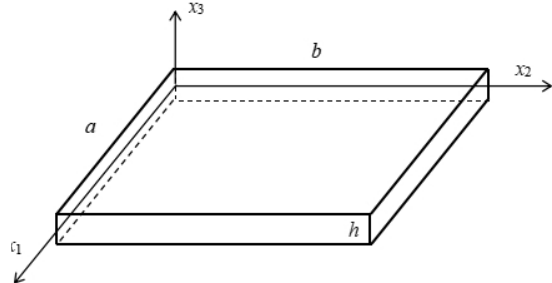


Figure 3. Rectangular plate $a \times b \times h$ in Cartesian coordinate system

In Eq. (15), the influence of mechanical loads (surface or volume forces) is not taken into account. Since it has been already explained that dynamic problems will not be considered in this case, Eq. (15) is reduced to a simple form

$$\nabla_1^2 w + (1+v)\alpha_t \tau_1 = 0. \quad (16)$$

Observe a free, supported plate of $a \times b \times h$ dimensions displayed in Fig. 3 and, in accordance with boundary conditions, apply a double finite Fourier transformation (defined already by the expression (4)). Since

$$\begin{aligned} \int_0^a \sin \alpha_n x_1 dx_1 &= \left. \frac{\cos \alpha_n x_1}{\alpha_n} \right|_0^a = \\ &= \frac{1 - \cos n\pi}{\alpha_n} = \begin{cases} 0, & n = 0, 2, 4, \dots \\ 2/\alpha_n, & n = 1, 3, 5, \dots \end{cases} \\ \alpha_n &= \frac{n\pi}{a} \quad \left(\alpha_m = \frac{m\pi}{b} \right). \end{aligned} \quad (17)$$

Eq. (16) is first reduced to the transformed expression

$$w_s(n, m) = \frac{4(1+v)\alpha_t \tau_1}{\alpha_n \alpha_m (\alpha_n^2 + \alpha_m^2)}, \quad (18)$$

and then applying inverse transformations, the solution for plate deflection is obtained in the form of a double infinite-order

$$\begin{aligned} w(x_1, x_2) &= C_1 \sum_{n=1,3}^{\infty} \sum_{m=1,3}^{\infty} \frac{\sin \alpha_n x_1 \sin \alpha_m x_2}{\alpha_n \alpha_m (\alpha_n^2 + \alpha_m^2)}, \\ C_1 &= \frac{16(1+v)\alpha_t \tau_1}{ab}. \end{aligned} \quad (19)$$

The last expression indicates that at a constant temperature gradient τ_1 , plate deflection does not depend on its thickness but only on the dimensions in the mid-plane.

Figure 4 shows the square plate deflection of $2\text{m} \times 2\text{m}$ dimensions calculated based on Eq. (19) along

mid-lines $x_1=x_2=1\text{m}$ for the gradient value τ_1 of $200^\circ\text{C}/\text{m}$. The analytically calculated value of the maximum displacement in the middle of the plate amounts to 0.92mm .

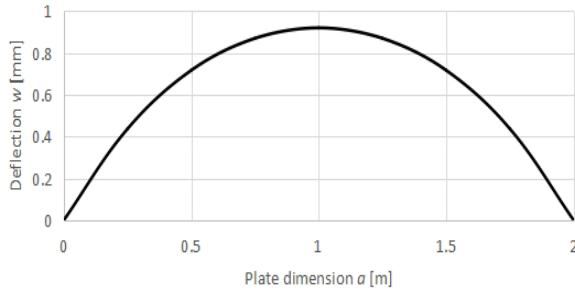


Figure 4. Deflection of the square plate 2m x 2m along midlines for $\tau_1=0.2^\circ\text{C}/\text{mm}$

The theory of thin plates yields expressions for maximum stresses in the form [14]:

$$\begin{aligned}\sigma_{11max} &= \mp \frac{Eh}{2(1-\nu^2)} \left[\frac{\partial^2 w}{\partial x_1^2} + \nu \frac{\partial^2 w}{\partial x_2^2} + (1+\nu) \alpha_t \tau_1 \right], \\ \sigma_{22max} &= \mp \frac{Eh}{2(1-\nu^2)} \left[\nu \frac{\partial^2 w}{\partial x_1^2} + \frac{\partial^2 w}{\partial x_2^2} + (1+\nu) \alpha_t \tau_1 \right], \\ \sigma_{12max} &= \mp \frac{Eh}{2(1+\nu)} \frac{\partial^2 w}{\partial x_1 \partial x_2}.\end{aligned}\quad (20)$$

Substituting (19) in expressions (20) gives maximum stress values in the analytical form

$$\begin{aligned}\sigma_{11max} &= C_2 \left[1 - \frac{16}{ab} \sum_{n=1}^{\infty} \sum_{m=1}^{\infty} \frac{(\alpha_n^2 + \nu \alpha_m^2) \sin \alpha_n x_1 \sin \alpha_m x_2}{\alpha_n \alpha_m (\alpha_n^2 + \alpha_m^2)} \right], \\ \sigma_{22max} &= C_2 \left[1 - \frac{16}{ab} \sum_{n=1}^{\infty} \sum_{m=1}^{\infty} \frac{(\alpha_m^2 + \nu \alpha_n^2) \sin \alpha_n x_1 \sin \alpha_m x_2}{\alpha_n \alpha_m (\alpha_n^2 + \alpha_m^2)} \right], \\ \sigma_{12max} &= \frac{8Eh\alpha_t\tau_1}{ab} \sum_{n=1}^{\infty} \sum_{m=1}^{\infty} \frac{\cos \alpha_n x_1 \cos \alpha_m x_2}{(\alpha_n^2 + \alpha_m^2)}, \\ C_2 &= \frac{Eh\alpha_t\tau_1}{2(1-\nu)}.\end{aligned}\quad (21)$$

Based on expression (21), it is evident that the highest normal stresses in a free-supported plate occur on its edges. The expression for tangential stress indicates that the stress equals zero for

$$\cos \frac{n\pi}{a} x_1 \cos \frac{m\pi}{b} x_2 = 0.$$

Since n and m are whole odd numbers, tangential stresses equal zero along the lines that halve the plate, i.e., for

$$\left(x_1 = \frac{a}{2}, x_2 \right), \left(x_1, x_2 = \frac{b}{2} \right).$$

Therefore, fig. 5 depicts the distribution of tangential stresses only for one-quarter of a considered square plate.

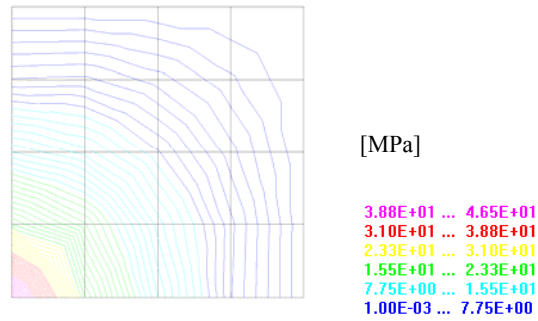


Figure 5. Analytically determined the distribution of tangential stresses

4. THE APPLICATION OF THE FINITE ELEMENT METHOD

The thin plate finite element was defined within the KOMIPS program package [11], and it was assigned the temperature of the mid-plane and the temperature gradient normal to the mid-plane. The temperature gradient is assigned in the direction of the finite element normal line. In order to compare the results obtained analytically (19) and numerically by applying FEM, a square plate was created of the same dimensions and loading as in the previous case.

Figure 6 shows plate deformation, and in accordance with the sign of the finite elements' normal line, a gradient of $\tau_1 = -0.2^\circ\text{C}/\text{mm}$ (a normal goes down) was assigned.

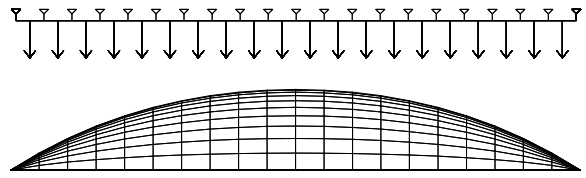


Figure 6. Direction of the finite elements' normal line and deformation of the square plate 2m x 2m

The finite element method was used to calculate a maximum deflection of 0.93 mm , which agrees well with the analytically obtained value (the difference is 1%).

Stress was checked for the plate with four clamped edges. Since, in that case, there is no displacement of the plate points, the stress obtained by the finite element method must agree with the theoretical stress from Eqs. (20). For the plate thickness of 100 mm and Modulus of elasticity of 210 GPa , normal stress amounts to

$$|\sigma_{11}| = |\sigma_{22}| = C_2 = 36 \text{ MPa}.$$

Since agreement between analytical and numerical calculations has been proved, only numerical calculations (being faster and simpler) were used for further analysis. The diagram in Fig. 7 shows the dependence of maximum deflection on the square plate dimensions in the mid-plane.

Figure 7 depicts the dependence of maximum deflection on plate thickness when the same temperature difference of 10°C is provided between two plate surfaces.

When the temperature difference between the plate's upper and lower surfaces is constant, only the tempera-

ture gradient changes with the factor h^{-1} so that the line from Fig. 8 corresponds to the hyperbole.

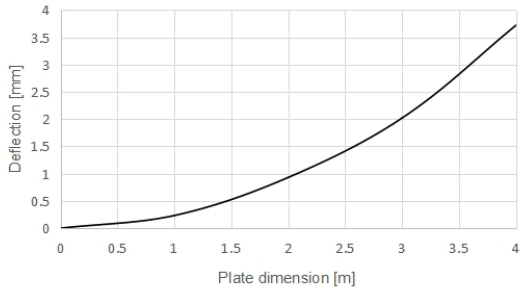


Figure 7. Square plate maximum deflection depending on its dimension a for $\tau_1=0.2^\circ\text{C}/\text{mm}$

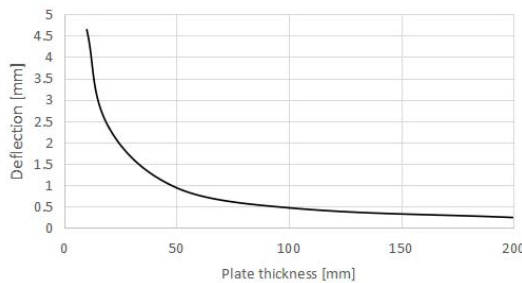


Figure 8. Square plate maximum deflection $a=b=2\text{m}$ depending on its thickness for a temperature difference of 10°C

5. TEMPERATURE GRADIENT DEPENDING ON THE MATERIAL OF THIN PLATE ELEMENTS

Observe the plate of dimensions $1\text{m} \times 1\text{m} \times 100\text{mm}$ with clamped edges. Also, observe the cylinder of medium diameter $d=1\text{m}$, length $l=3\text{m}$, and thickness $\delta=100\text{mm}$, also with clamped edges, shown in Fig. 9. Elements of plate and cylinder are loaded with the same temperature gradient of $200^\circ\text{C}/\text{m}$.

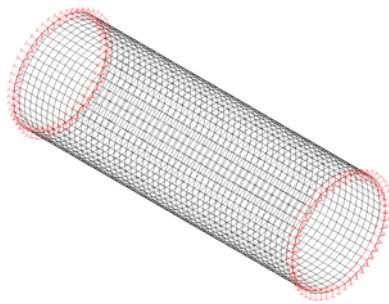


Figure 9. A numerical computational model of cylinder supports (boundary conditions)

Observe the plate and cylinder are made whole of one of three materials: reinforced concrete, carbon steel, and brass (CuZn30). Material characteristics used in calculations are given in Table 2.

Firstly, observe the method and speed of heating of plates when the temperature difference between the upper and lower sides is set to 20°C . In the diagrams in Fig. 10, the mid-plane temperature change for a concrete and brass plate is shown. The diagrams were obtained on the basis of analytical calculations using equation (9).

Table 2. Material characteristics

Material	Concrete	Carbon steel	Brass
Elasticity Modulus E [GPa]	30	210	100
Poisson's coefficient ν	0.2	0.3	0.37
Thermal conductivity λ [W/mK]	1.51	50.2	105.8
Specific heat C [J/kgK]	840	470	377
Material density ρ [kg/m ³]	2500	7800	8600
Coefficient of thermal expansion α [K ⁻¹]	$1.2 \cdot 10^{-5}$	$1.2 \cdot 10^{-5}$	$1.9 \cdot 10^{-5}$

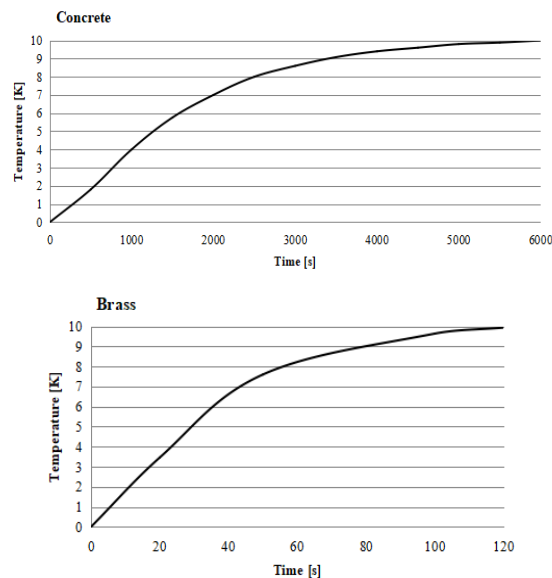


Figure 10. The mid-plane temperature change for a concrete and brass plate

A stationary temperature field in a concrete plate is established in about 100 minutes, in a steel plate in about 4 minutes, and in a brass plate in only about 2 minutes.

Since the displacements of the plate with clamped edges, loaded in this way, are equal to zero, the expression for theoretical stress based on equation (21) is

$$|\sigma_{11\max}| = |\sigma_{22\max}| = \frac{Eh\alpha_t\tau_1}{2(1-\nu)}, \quad \tau_{12} = 0, \quad (22)$$

which gives a stress of 4.5 MPa for the concrete plate, 36 MPa for the steel plate, and 30.2 MPa for the brass plate. The von Mises stress σ_{eqv} by the plane stress theory is defined by the following equation

$$\sigma_{\text{eqv}} = \sqrt{\sigma_{x_1}^2 + \sigma_{x_2}^2 - \sigma_{x_1}\sigma_{x_2} + 3\tau_{x_1x_2}^2}, \quad (23)$$

so the value of the equivalent stress in this load case is equal to the maximum values of the normal stress. Calculations performed using the finite element method give exactly the same stress values. The same stress values are obtained for the cylinder shown in Figure 9.

If the plate is only freely supported (Figure 11), its deformations occur in a way that the maximum displacements of the midpoint (obtained using the finite

element method) are: f_{\max} (concrete)=0.2 mm, f_{\max} (steel)= 0.23 mm, f_{\max} (brass)= 0.4 mm.

If the temperature in the middle plate plane of $\theta_0=50^\circ$ is added to the calculation, the strain and stress values are obtained by the finite element method and given in Table 3.

Tabela 3. Maximum deflections and equivalent stresses

Material	f_{\max}	Compressive stress in plate mid-plane	Eqv. Stress [MPa]
Concrete	0.211 mm	22.5 MPa	29.7 ÷ 31.2
Steel	0.286 mm	180 MPa	239 ÷ 248
Brass	0.382 mm	151 MPa	201 ÷ 208

Using the finite element method, equivalent stresses are calculated using the Maxwell–Huber–Hencky–von Mises criterion. Stress distribution, as well as deformation, is the same in all the plates made of different materials and is given in Fig 11.

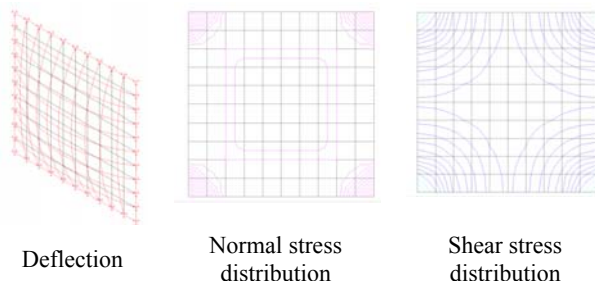


Figure 11. Deformation. Normal stress distribution and shear stress distribution in a thin plate model

The finite element method calculation of a cylinder with clamped edges loaded only with a linear temperature gradient for all three materials shows a curling tendency. For a temperature gradient of $200^\circ\text{C}/\text{m}$, the displacements are small, and the appearance of the deformed cylinder is given in Fig. 12.

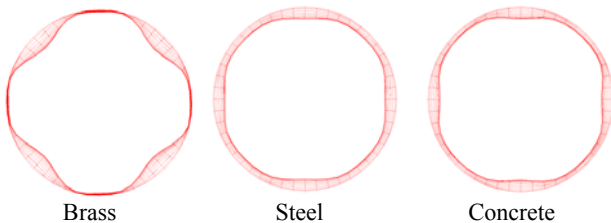


Figure 12. Deformation of a cylinder loaded only with a linear temperature gradient

6. SOLVING PRACTICAL ENGINEERING PROBLEM USING FINITE ELEMENT

Previous considerations are significant for solving geometrically more complex problems when the finite element method has to be used. Problem-solving commences by defining the temperatures on the plate element's upper and lower surfaces.

At first, observe a flat plate and define heat flux based on the expression for heat transmittance through flat walls. Let the steel plate be of thickness $h=\delta=100$ mm and let the air of the temperature of $T_{f1}=120^\circ\text{C}$ and velocity of approx. 20 m/s flow over its upper surface, and air of the temperature $T_{f2}=20^\circ\text{C}$ and of the same

velocity flow over its lower surface. Heat transfer coefficients obtained based on an empirical formula amount to $\alpha_1=\alpha_2=45\text{W/m}^2\text{K}$. Heat flow is calculated using the expression (24) [15]

$$\phi[\text{W/m}^2] = \frac{T_{f1}-T_{f2}}{\frac{1}{\alpha_1} + \frac{\delta}{\lambda} + \frac{1}{\alpha_2}} \quad (24)$$

and amounts to 2153W/m^2 . In that case, the plate's upper surface temperature is 72.15°C , and of the lower surface, 67.85°C . The mid-plane temperature is $\tau_0=70^\circ\text{C}$, whereas the temperature gradient normal to the mid-plane is $\tau_1=43^\circ\text{C/m}$.

For metal structures that have high thermal conductivity λ (steel, aluminum, copper, and their alloys), the temperature gradient τ_1 has a comparatively small value so that it can be neglected in some calculations. For all structural parts built of non-metals, the temperature gradient is very high, and it is mandatory to introduce it in calculations.

If the material of the observed plate were reinforced concrete or quartz glass, for the same boundary conditions, the mid-plane temperature would amount to 70°C and the linear gradient to approx. 600°C/m , while for the plate made of plaster, brick, or concrete, the gradient would be approx. 800°C/m .

In order to more clearly show the importance of the material characteristics of the construction on its behavior under the influence of temperature, observe the already described cylinder whose inner and outer diameters are $d_u=0.95$ m and $d_s=1.05$ m. Let the air at a temperature of $T_u=100^\circ\text{C}$ and at a speed of $v_u=15$ m/s flow inside the cylinder. Let the air at the temperature $T_s=20^\circ\text{C}$ and at the speed of $v_s=2$ m/s flow at the outer side of the cylinder. Heat transfer coefficients α_u and α_s can be determined using empirical formulas, and for this case, their values are $\alpha_u=40\text{ W/m}^2\text{K}$ and $\alpha_s=26\text{ W/m}^2\text{K}$. The heat flux ϕ [W/m] is calculated based on the equation (25) from the literature [15]

$$\phi = \frac{T_u - T_s}{\frac{1}{d_u \pi \alpha_u} + \frac{1}{2\pi\lambda} \ln \frac{d_u}{d_s} + \frac{1}{d_s \pi \alpha_s}} \quad (25)$$

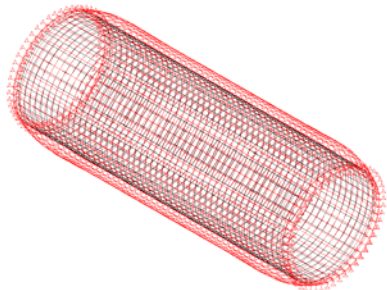
The temperatures of the inner and outer sides of the cylinder T_u and T_s are calculated and given in Table 4.

Table 4. Characteristics cylinder temperatures

Material	Concrete	Steel	Brass
Inner side temperature T_u	78.08°C	67.1°C	66.8°C
Outer side temperature T_s	50.51°C	65.75°C	66.2°C
Middle plane temperature τ_0	64.3°C	66.44°C	66.5°C
Linear temperature gradient τ_1	276°C/m	13.8°C /m	6°C/m

When considering the temperature gradient included in the numerical finite element method calculation, one should take care of the normal direction of the surface element. Since in the shown model, the normal of the surface element goes outwards, τ_1 is considered with a

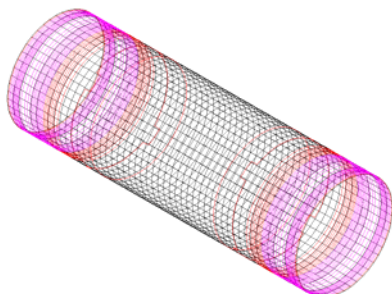
minus sign. In this numerical example, the edges of the cylinder are freely supported (in all three directions), as shown in Fig. 13. The deformation field has the same shape for all considered materials and is given in Fig. 13, as well as the corresponding values of the maximum displacements.



Concrete Steel Brass
 $f_{\max} = 0.5\text{mm}$ $f_{\max} = 0.5\text{mm}$ $f_{\max} = 0.9\text{mm}$

Figure 13. Deformation of the cylinder under the thermal loading

Figure 14 shows the equivalent stress distribution field as well as von Misses stress values for all three cases. It is clear that the stresses are the highest at the places of structure supports.



Concrete [MPa]	Steel [MPa]	Brass [MPa]
1.91E+01 ... 2.29E+01	1.14E+01 ... 1.53E+01	1.14E+02 ... 1.37E+02
1.53E+01 ... 1.91E+01	1.14E+01 ... 1.53E+01	9.13E+01 ... 1.14E+02
1.14E+01 ... 1.53E+01	7.63E+00 ... 1.14E+01	6.85E+01 ... 9.13E+01
7.63E+00 ... 1.14E+01	3.82E+00 ... 7.63E+00	4.57E+01 ... 6.85E+01
3.82E+00 ... 7.63E+00	0.00E+00 ... 3.82E+00	2.28E+01 ... 4.57E+01
0.00E+00 ... 3.82E+00	0.00E+00 ... 3.82E+00	0.00E+00 ... 2.28E+01

Figure 14. Equivalent stress distribution field in considered cylinder model

When analyzing the calculated stress field, one should be very careful due to the different characteristics of the considered materials. Depending on the method of production, the tensile strength of brass ranges from the usual 150 MPa and even up to 440 MPa, while the tensile strength of structural steels is from 340 MPa to 850 MPa. That is why these materials can withstand thermal loads very well. Reinforced concrete has completely different characteristics. The standardized compressive strength of reinforced concrete ranges from 10 to 60 MPa, while the tensile strength is only about 10% of the compressive strength. Due to the small value of thermal conductivity λ , the temperature gradient τ_1 is very significant here. As it causes bending, tensile stresses also appear, and the allowable value of tensile stress is below 6 MPa. Based on equation (22), the concrete can withstand the maximum temperature difference between the two sides of the plate in an amount of about 27°C.

7. CONCLUSION

The paper analytically proves the justification of the assumption that the temperature field of thin plate elements is defined through mid-plane temperature and linear temperature gradient normal to the mid-plane. In an analytical closed form, applying the method of integral transformations, the thin plane deflection was determined to be caused by the constant temperature gradient. It is shown that the deflection does not depend on the plate thickness but only on the dimensions in the mid-plane. Also, the corresponding stress field was analytically determined. The same problem was solved numerically, applying the thin plate finite element, where the temperature field is described using temperature in the middle plane and appropriate temperature gradient. The agreement of obtained results confirmed the usage of this finite element. The paper also presents the dependence of the plate deflection on its thickness at constant temperature differences between the upper and lower plate surfaces. Since temperature gradient depends most on the type of material, it is shown that its influence is of great importance for non-metal parts of machines and building structures. The temperature gradient can be neglected in most calculations for structures made of materials with high thermal conductivity. But for non-metallic constructions, especially concrete ones, the temperature gradient is extremely important and must be taken into account in the calculation.

ACKNOWLEDGMENT

The results presented are the results of the research on Projects TR35040 and TR35011, supported by the Ministry of Science, Technological Development and Innovation of the Republic of Serbia, contract no. 451-03-47/2023-01/200105 from 03.02.2023.

REFERENCES

- [1] Gaćesa, B., Maneski, T., Milošević-Mitić, V., Nestorović M., Petrović, A.: Influence of furnace tube shape on thermal strain of fire-tube boilers, Thermal Science, Vol. 18, Suppl. 1, pp. S39-S47, 2014.
- [2] Rajić, M., Banić, M., Živković, D., Tomić, M., Mančić, M.: Construction optimization of hot water fire-tube boiler using thermomechanical finite element analysis, Thermal Science, Vol. 22, Suppl. 5, pp. S1511-S1523, 2018.
- [3] Abdullah, O., Schlattmann, J., Lytkin, M.: Effect of surface roughness on the thermoelastic behaviour of friction clutches, FME Transactions Vol. 43, pp. 241-248, 2015.
- [4] Hemanth, J., Yogesh, K.B.: Finite element analysis (FEA) and thermal gradient of a solid rectangular fin with embossing's for aerospace applications, Advances in Aerospace Science and Technology, Vol. 3, pp. 49-60, 2018.
- [5] Shi, Y., Shen, H., Yao, Z., Hu, J.; Temperature gradient mechanism in laser forming of thin plates, Optics&Laser Technology, Vol 39, pp. 858-863, 2007.

- [6] Kiran, B., Mishra, K., Singh, Y.R., Nagaraju, D.: Structural and thermal analysis of Butt Joint GTAW of similar and dissimilar material with distinct groove angles through simulation and mathematical modeling, *FME Transactions*, Vol. 48, pp. 667-680, 2020.
- [7] Khazaenejad P., Usmani A.S., Lagrouche O.: Temperature-dependent nonlinear behaviour of thin rectangular plates exposed to through-depth thermal gradients, *Composite structures*, Vol.132, pp. 652-664, 2015.
- [8] Allam, M., Tayel I.: Thermal effects on transverse vibrations of non-homogeneous rectangular thin plate subjected to a known temperature distribution, *Transactions of Canadian Society for Mechanical Engineering*, Vol. 44, No. 3, 2020.
- [9] Kuzmanović, M., Savić, Lj., Mladenović N.: Thermal-stress behaviour of RCC gravity dams, *FME Transactions*, Vol. 43, pp. 30-34, 2015.
- [10] Xu, J., Yuan, H.: Estimate of temperature gradients of thin-walled structures under thermomechanical fatigue loading, *American Institute of Aeronautics and Astronautics*, Vol. 60, No. 9, 2022.
- [11] Maneski, T.: *Computer modeling and structure analysis*, Faculty of Mech. Eng., University of Belgrade, 2000.
- [12] Ćukić, R., Naerlović-Veljković, N., Šumarac, D.: *Thermoelasticity*, Faculty of Mech. Eng., University of Belgrade, 1993. (in Serbian)
- [13] Milošević-Mitić, V.: Temperature and stress fields in thin metallic partially fixed plate induced by harmonic electromagnetic wave, *FME Transactions* Vol. 31, pp. 49-54, 2003.
- [14] Milošević-Mitić, V.: *Magneto-thermo-elastic bending of thin plates*, Zadužbina Andrejević Publications, Belgrade 1999. (in Serbian)
- [15] Vasiljević B., Banjac M.; *Handbook of thermodynamics*, Faculty of Mech. Eng., University of Belgrade, 2017. (in Serbian)

**УТИЦАЈ ТЕМПЕРАТУРСКОГ ГРАДИЈЕНТА
НА САВИЈАЊЕ ТАНКИХ ПЛОЧА**

**В. Милошевић-Митић, А. Петровић,
Н. Анђелић, М. Јовановић**

У оквиру теорије термоеластичности уобичајено је да се поље температуре танких плача дефинише преко температуре у средњој равни и линеарног градијента температуре управно на средњу раван. У раду је прво анали-тички доказана оправданост те претпоставке у машинским конструкцијама. Затим је у затвореном аналитичком облику, применом методе интегралних трансформација, одређен угиб танке плаче који изазива константан градијент температуре. Показано је да у том случају угиб плаче не зависи од њене дебљине већ само од димензија у средњој равни. Аналитички одређене вредности упоређене су са одговарајућим вредностима добијеним применом одговарајућег кона-чног елемента танке плаче. Овај коначни елемен-т дефи-нисан је и испрограмиран у оквиру програмског пакета Комипс. Утицај температу-рског градијента на понашање конструкција највише зависи од врсте материјала, па је у раду анализирано понашање не-ких конструктивних елемената од месинга, челика и бетона.